

Single element SAR measurements in a multi-transmit system

U. Katscher¹, C. Findekle¹, and T. Voigt¹

¹Philips Research Europe, Hamburg, Germany

Introduction: A central issue of parallel RF transmission is the SAR management in the framework of patient safety. The additional degrees of freedom available in parallel transmission hamper straight-forward global / local SAR estimations as applied for single channel transmit systems (see, e.g., [1]). Recently, a method has been presented to estimate SAR from the acquired B1 maps [2]. However, this method was restricted to quadrature volume coils due to difficulties distinguishing the contribution from RF transmission (TX) and signal reception (RX) to the spatial phase distribution in the obtained images. This study presents a method to separate these two phase contributions, and thus, enables SAR estimation not only for quadrature volume coils, but also for single elements of a TX array.

Theory: Given the complex B1 map of a certain coil array element, the electric properties $\underline{\kappa} \equiv \omega \varepsilon + i \sigma$ (ε = permittivity, σ = conductivity, ω = Larmor frequency) of the investigated body area can be reconstructed using “Electric Properties Tomography” (EPT), see Eq. (1) [3]. Subsequently, the corresponding local SAR distribution can be estimated using Eq. (2) [2]. The required amplitude of B1 can be mapped with standard B1 mapping techniques (see, e.g., [4]). On the other hand, standard MR images acquire only relative phase distributions $\varphi_n = \tau_n + \rho$, i.e., the sum of the spatial phase distribution from RF transmission τ_n and signal reception ρ . The index $n \leq N$ refers to the TX element n of the N -element array used. However, relative phases are not sufficient for the described SAR estimation due to the calculus operations applied in (1,2). To obtain the required absolute phase of B1 of a certain TX element, the following procedure is tested. Accurate EPT reconstructions for two different transmit elements n, m should yield the same $\underline{\kappa}_n = \underline{\kappa}_m = \underline{\kappa}$. Thus, ρ can be determined iteratively until Eq. (1) yields the same $\underline{\kappa}$ for both transmit elements. Afterwards, it is straight-forward to obtain τ_n and τ_m from φ_n and φ_m , respectively, allowing suitable SAR estimations for channels n and m , and analogously for the remaining TX elements.

Methods: The described SAR mapping method was tested using a 3T system (Philips Achieva, Best, Netherlands), equipped with $N = 8$ independent TX/RX elements [5,6]. B1 amplitude mapping was performed using MTM [7] based on multiple AFI scans [4]. Relative B1 phase maps were based on the FFE images obtained in the framework of MTM with subsequent B0 inhomogeneity corrections. Absolute phase maps were derived by the above-described iteration fitting ρ to a 4-order polynomial using a simplex algorithm. The resulting SAR maps are compared with corresponding simulations using Concept II (TU Hamburg-Harburg, Germany). Cylindrical phantoms (height = 6 cm, $\varnothing = 6$ cm), placed 8 cm to the right off-iso-center, were investigated containing six different phantom fluids with ε and σ covering roughly the physiologic range.

Results: Local SAR distributions for two example elements (positions 2 o'clock and 7 o'clock) are shown for a phantom with $\varepsilon_r = 74$ and $\sigma = 0.5$ S/m (Fig. 1). The simulated SAR is compared with the reconstructed SAR using the above-described separation of TX and RX phase contributions as well as ignoring the RX phase contribution. The absolute scale corresponds to a mean total B1 of $10 \mu\text{T}$ and a duty cycle of 100%. The difference between $\underline{\kappa}_n$ and $\underline{\kappa}_m$ converges after 10-15 iteration steps to typically $|\underline{\kappa}_n - \underline{\kappa}_m| = 0.1\text{-}0.2$ S/m (Fig. 2).

Discussion & Conclusion: The high correlation between simulated and experimental results underlines the feasibility of the proposed method to map local SAR for single TX elements. The result might indicate that the proposed SAR mapping could play a role in patient-individual SAR management in parallel RF transmission. Future studies have to clarify if this SAR mapping is applicable also *in vivo*, and if it is superior to the currently applied patient-model-based SAR management. Besides SAR management, the presented separation of TX and RX phase might also be useful for other areas in MRI, e.g., RF coil characterization.

References: [1] Graesslin I et al., ISMRM 14 (2006) 2041 [2] Katscher U et al., IEEE Trans Med Imag 28 (2009) 1365 [3] Voigt T et al., ISMRM 18 (2010) 2865 [4] Yarnykh VL, MRM 57 (2007) 192 [5] Graesslin I et al., ISMRM 14 (2006) 129 [6] Vernickel P et al, MRM 58 (2007) 381 [7] Voigt T et al., MRM 64 (2010) 725

$$\oint_{\partial V} \nabla \underline{B}_1^+ \cdot \underline{d}\underline{a} / \omega^2 \mu \int_V \underline{B}_1^+ \cdot \underline{d}V = \underline{\kappa} \quad (1)$$

$$\text{SAR} \sim \sigma \underline{E}^2 = \sigma \left(\nabla \times \underline{B}_1 / \omega \underline{\kappa} \right)^2 \quad (2)$$

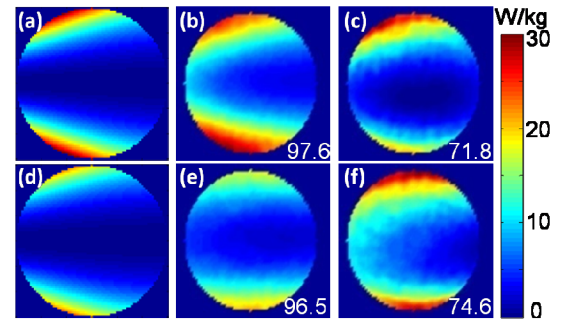


Fig. 1: Local SAR maps of a phantom ($\varepsilon_r = 74$, $\sigma = 0.5$ S/m). Upper / lower row: different TX array elements. (a/d) Simulated SAR, (b/e) measured SAR, TX/RX phase separated, (c/f) measured SAR, RX phase ignored. Numbers indicate the correlation with corresponding simulated SAR.

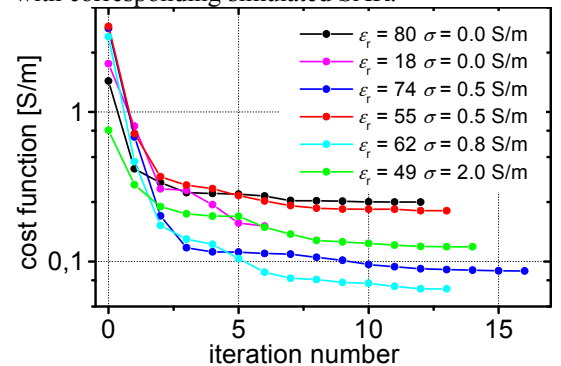


Fig. 2: Difference of two example channels' $\varepsilon\omega$ and σ for different phantoms, decreasing during the iteration separating TX/RX phases.